

Implications of double composite liner behaviour for PFAS containment

R. Kerry Rowe¹, and Linxue Zhao²

¹ Professor, Queen's University, Kingston, ON, Canada, email: kerry.rowe@queensu.ca

² PhD Student, University of Sydney, NSW, Australia, email: linxue.zhao@sydney.edu.au

ABSTRACT

Parameters controlling leakage through composite liners with either a geosynthetic clay liner (GCL) or compacted clay liner (CCL) are established through a calibration exercise and found to provide a good description of observed leakage through the primary liner of a double-lined system both with and without a leak location survey. In contrast, the leakage through the secondary liner of the Ontario double-liner system is very small with the use of a GCL and substantially lower than with a single-liner system, for both a GCL and CCL as part of a composite liner.

Keywords: Geosynthetics, Landfill, Composite liners, Leakage, PFAS

1 INTRODUCTION

Composite liners, typically a high density polyethylene (HDPE) geomembrane (GMB) over a geosynthetic clay liner (GCL) or compacted clay liner (CCL), have been extensively used in the disposal of municipal solid waste (MSW; Rowe et al., 2004; Rowe, 2020). They have generally performed very well for contaminants of concern over the last century. Some jurisdictions have traditionally mandated double-lined systems for MSW landfills (e.g., New York State; Rowe and Barakat, 2021) while others have required double-lined systems for anything but small landfills (MoE, 1998). The identification of significant levels of per- and polyfluoroalkyl substances (PFAS) in waste and landfill leachates necessitates a re-evaluation of these designs.

PFAS are manufactured compounds comprised of a carbon chain where some or all the hydrogen atoms have been replaced with fluorine atoms (Buck et al. 2011, U.S. Department of Health and Human Services 2022). The chemical bond between the carbon and fluorine atoms of these molecules makes them extremely stable and difficult to degrade. PFAS have had many beneficial uses (U.S. Department of Health and Human Services 2022, Milinovic et al. 2015; Bouazza 2021). However, the strong carbon-fluorine bond also makes them persistent “forever chemicals”. PFAS have been extensively used in industrial and consumer goods including surfactants, repellents, and lubricants. The products containing PFAS span from firefighting foams to common domestic products such as non-stick cookware, to carpets, clothing, furniture, food packaging, and cosmetics (ATSDR 2015, CELA 2019, CONCAWE 2016, EPA 2003, Ahrens 2011, NTP 2016, Cousins et al. 2016, EPA 2017, Rowe and Barakat 2021, U.S. Department of Health and Human Services 2022). Research has indicated that high levels of PFAS in the human body may result in high cholesterol levels, changes to the function of the liver, reduced immune system function, a higher probability of kidney and testicular cancer, and thyroid disease (Steenland et al. 2010, Jones 2016, Garcia 2017). This, combined with the fact that there is already a significant amount of PFAS in existing landfills, raises the following questions: (I) how well are PFAS contained in existing single-lined and double-lined landfills? and (II) how should future landfills be designed to ensure adequate containment?

Di Battista et al. (2020) provided evidence to suggest that modern polyethylene geomembranes used in landfill liners are likely to be an excellent barrier to diffusion to per-fluoroalkyl acids such as per-fluorooctanoic acid (PFOA) and per-fluorooctanesulfonic acid (PFOS) commonly found in landfill leachate. However, an assessment of PFAS risk to groundwater also needs to consider advective transport due to the leakage of leachate through holes in the geomembrane. Hence, following from Di Battista et al. (2020), Rowe and Barakat (2021) demonstrated the potential for leakage through holes in

a geomembrane of a single composite liner could allow levels of PFOS into groundwater that would be unacceptable in many jurisdictions. The study by Rowe and Barakat (2021) considered several specific combinations of parameters that control leakage but did not take a statistically based approach to leakage and the combination of factors that can affect leakage. As a first step towards full evaluation of the potential for PFAS contamination to groundwater below landfills, the objective of this paper is to apply a probabilistic approach to evaluating the leakage through single composite liners and a double-lined system. This objective is achieved in three stages:

1. Compare the leakage rates from an analytical equation described with those from the finite element model to verify the applicability of the former and the mesh refinement of the latter. Both the analytical and numerical models are used to calibrated parameters against available experimental data from many landfill cells to generate realistic probability distributions of hydraulic conductivities of the liner and the transmissivities of the GMB-liner interfaces.
2. Using these distributions, Monte Carlo realisations of steady-state hydraulic flow through a single-liners are obtained using both the analytical model and finite element model, to derive probability distributions of leakage rates. In these simulations, uncertainties in defects in geomembranes wrinkles (“holed wrinkles”), the length (L_w) of holed wrinkles, the head difference (Δh) due to uncertainty in the leachate level and water level below the composite liner are considered, in addition to uncertainties in the hydraulic properties of liners.
3. The process is repeated for a double liner using the verified analytical approach. Because of the very high level of mesh refinement and large number of elements required to model very thin transmissive layers, geomembranes, and GCLs together with the attenuation layers and the aquifer given number of wrinkles with holes and the large lateral extent of the landfill, the computational time for large number of runs needed for conventional Monte Carlo analyses was excessive and so numerical methods were not used for the double liner Monte Carlo analyses.

2 LEAKAGE THROUGH COMPOSITE LINERS

HDPE GMBs experience significant thermal expansion and consequent wrinkling (waves) upon heating (e.g., Giroud and Peggs 1990; Giroud and Morel 1992; Pelte et al. 1994; Giroud 1995; Rowe 1998; Koerner et al. 1999; Touze-Foltz et al. 2001). However, there was very little data regarding actual wrinkle dimensions that could be used to quantify leakage for realistic wrinkle geometries until the studies by Take et al. (2007), Chappel et al. (2012a,b), and Rowe et al. (2012a,b) discussed below.

Based on studies at the full-scale Queen’s University Environmental Liner Test Site (QUELTS) located north of Kingston, Canada, it has been reported to be rare that thermal expansion induced wrinkles (“wrinkles” in this paper) exceed 0.2 m in height and 0.5 m width due to solar radiation (Rowe *et al.* 2012a). The average wrinkle height has been found to be about 0.06 m and the width ($2b$) between about 0.2 m and 0.25 m with an average of 0.20 m and 0.22 m on the base and slope respectively with a standard deviation of 0.04 m in both cases (Rowe *et al.* 2012a). Early in the day, wrinkles start to form independently and the connected wrinkle length increases slowly to about 200 m with increasing area of wrinkles until about 8% of the area is wrinkled. The wrinkles then begin to interconnect. The length of the connected wrinkle grows rapidly with further increase in the area under wrinkles reaching over 2000 m when 20-30% of the site is wrinkled (Rowe *et al.* 2012b). To keep the connected wrinkle length below 200 m during the summer construction season, the GMB would generally need to be covered before 8-9 am or after 4-5 pm. Thus, as indicated by Rowe (2012), with 2.5 to 5 holes/ha, if GMB is covered between dawn and 9am, there is a reasonable probability that, there would be at least one hole in a connected wrinkle of length $L_w \leq 200$ m. If covered later in the day the probability of a hole in a wrinkle increases as does the length of the connected wrinkles. If the geomembrane is covered near 1:30 pm, assuming 5 holes/ha, there would be a 50% probability that a hole would align with a wrinkle with $L_w \geq 1500$ m assuming holes are random. However, as noted by Gilson-Beck (2019) and Rowe (2020), wrinkles are preferentially damaged and it is hard to find holes in wrinkles with electrical leak location methods without a conductive geomembrane; thus, attention is focused on holes in wrinkles.

Wrinkles locked in after covering may get smaller as the waste is placed but do not go away with typical drainage layer materials and pressures up to 1000 kPa (Gudina and Brachman 2006, 2011; Brachman and Gudina 2008). Thus, wrinkles provide both a potential source for holes and transmission of flow through the hole and can also serve to dam-up and conduct the leachate to a hole in a wrinkle with leachate levels building up to the height of the wrinkles (i.e., up to 0.2 m; Rowe et al. 2012a).

Using a low-altitude aerial photogrammetric system developed by Take *et al.* (2007), Chappel *et al.* (2012a,b) and Rowe *et al.* (2012a,b) have quantified wrinkles at nine different sites in eastern Canada. From these studies, it can be concluded that although wrinkles may reach heights of 0.2 m or more and widths up to 0.5 m on occasions, based on a detailed analysis of a very large number of wrinkles at nine sites at different times of day, wrinkles are typically about 0.06 m high with an average wrinkle width (2*b*) of 0.20–0.23 m over a GCL and 0.24–0.32 m over a CCL. The typical width does not change significantly over most of the day. The connected length of thermal expansion induced wrinkles varies substantially with time of day from negligible thermal wrinkles at night, less than 200 m if covered before 9am, but between 2,000 and 10,000 m if covered towards the middle of the day, with up to about 30% of the area being below a wrinkle.

Rowe (1998) developed an equation to predict leakage through a hole in a geomembrane coincident with (or adjacent to) a wrinkle:

$$Q = 2 L_w [k_b b + (k_a D \theta)^{0.5}] \Delta h / D \quad (1)$$

Where the symbols are defined in Table 1. Results from Equation 1 (the Rowe (1998) Equation) were compared with those from a finite-element program (the Soil Pollution Analysis System, SPAS; El-Zein and Balaam, 2012) to validate the equation and check the finite element mesh. Then both Equation 1 and SPAS were used (as cross-verification using independent random number generators) to generate probability distributions of hydraulic conductivities and interface transmissivities of liners by calibrating the leakage predictions to experimental data. Once the hydraulic parameters were obtained, they were used to establish the wrinkle distribution associated with good construction quality assurance and the absence or presence of an Electrical Leak Location Survey (ELLS: Gilson-Beck, 2019). For simulations of single-liners in Section 4, a finite element solver, the Soil Pollution Analysis System (SPAS), has been used (El-Zein and Balaam, 2012). In Section 5, the double-liner simulations were performed using the analytical approach (Equation 1) for both the primary and secondary liner implemented so as to allow consideration of $\Delta h_{Primary}$ in the primary liner due to uncertainty in the leachate level, $\Delta h_{Secondary}$ in the secondary liner. This uncertainty is related to uncertainty in the water level below the composite liner, in addition to uncertainties in hydraulic properties of liners assuming that: (i) the leakage through the secondary liner is always less than or equal to that through the primary liner for each simulation of the double-lined system, (ii) L_w is the same for both liners, and (iii) there is an effective secondary leachate collection system for controlling head on the secondary liner and removal of leakage through the primary liner in excess of the leakage through the secondary liner.

Table 1. Notation

AL	Attenuation layer	h_a	Height above bottom of AL to water level (m)
AM	Arithmetic mean	k_a	Hydraulic conductivity of a GCL where the GMB is in good contact with the GCL (m/s)
a_o	Base value		
b	Half-width of a wrinkle (m)	k_b	Hydraulic conductivity of GCL below a wrinkle (m/s)
CCL	Compacted clay liner	k_{AL}	Hydraulic conductivity of AL (m/s)
D	Thickness of the clay liner (m)	$ln(GSD)$	Standard deviation of a lognormal distribution
ELLS	Electrical leak location survey	lphd	Liters per hectare per day
GCL	Geosynthetic clay liner	L_w	Length of holes wrinkle per hectare (m/ha)
GM	Geometric mean	Q	Leakage rate (m ³ /s) or (lphd)
GMB	Geomembrane	Q_{95}	95% probability $Q < Q_{95}$
Δh	Head loss across the liner (m)	θ	Transmissivity of GMB/clay liner interface (m ² /s)

3. CALIBRATION TO OBSERVED LEAKAGE THROUGH A PRIMARY COMPOSITE LINER

3.1 Data from Beck (2015).

The establishment of realistic parameters to use for evaluating likely leakage rates and ultimately the probability of PFAS concentrations exceeding allowable levels in the groundwater, requires data for verification. This subsection describes the data set that was used and discusses the parameters required to be compatible with that data set.

The best available data arises from New York State's requirement for double-lined MSW landfills together with annual reporting of actual leakage through the primary liner. Beck (2015) collected and analysed this leakage rate data from 122 discrete landfill cells where there had been good construction

quality control but no electrical leak location survey (no ELLS). Leakage rate data was also analysed for 60 discrete landfill cells where a dipole method electrical leak location survey was conducted (ELLS). Based on the data, a plot of the probability of leakage exceeding a given value was constructed. This data is given in Figure 1 for no ELLS and in Figure 2 with a dipole ELLS. The landfills for which data is given in Figures 1 and 2 involved composite liners comprised of a GMB over a GCL (GMB/GCL) and a GMB over a CCL (GMB/CCL).

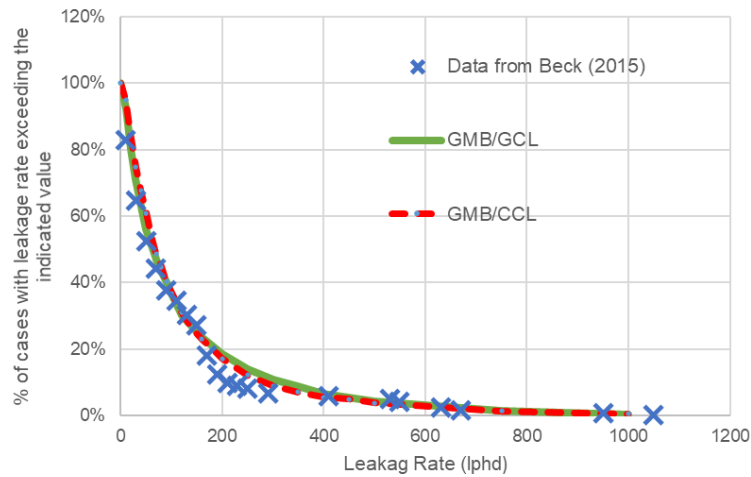


Figure 1. Probability (as a percentage of the 122 landfills cells for which data is reported by Beck, 2015) that a given leakage rate is exceeded together with calculated rates for GMB/GCL and GMB/CCL.

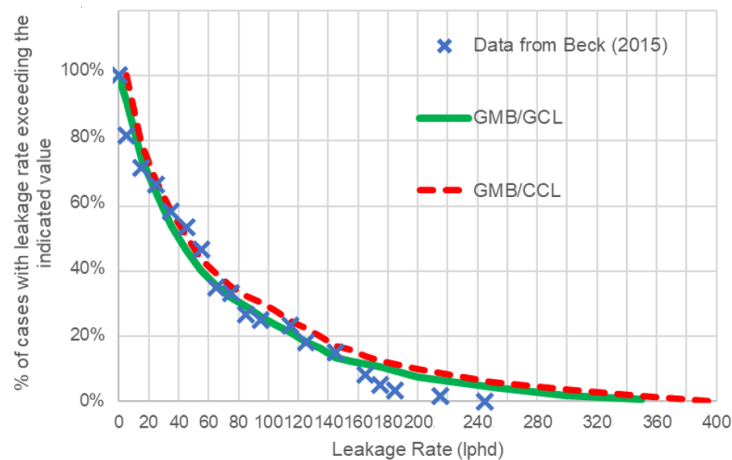


Figure 2. Probability of leakage exceeding a given value after a dipole ELLS based on 60 landfills cells reported by Beck (2015) together with calculated rates for GMB/GCL and GMB/CCL.

3.2 GCL Parameters to fit observed data.

The data for the case with no ELLS and with ELLS could be reasonably approximated with a Monte Carlo simulation (Figures 1 and 2) using the parameters given in Table 2 assuming a base value, a_0 , to which was added a value from a lognormal distribution with a geometric mean (GM) and standard deviation (ln(GSD)) as indicated. Each parameter had a different effect on the resulting curves in Figures 1 and 2 and hence the parameters were established by optimising the fit of the consequent curve to the data. The characteristic of the data points derived from these distributions are given in Table 3. The same GCL parameters (Table 2) were used both without and with an ELLS. The GCL in contact with the GMB, k_a , was subject to significant vertical stress due to the weight of the overlying waste and the distribution (Figure 3) that best fit the data had an average (AM) hydraulic conductivity of 5.8×10^{-11} m/s with most values falling between 0.2×10^{-11} and 10×10^{-11} m/s.

The hydraulic conductivity of the GCL was subject to cation-exchange from interaction with the leachate and this affects both k_a and k_b . The effect of cation-exchange on k_a of the GCL is offset by self-healing under the applied stress of the waste over the geomembrane, giving the relatively low values in Figure 3 and Table 3. However, for the GCL beneath the wrinkle there is no opportunity for self-healing because the effective stress is essentially zero below the wrinkle remaining after compression. Thus, the ratio $[k_b/k_a - 1]$, had a GM of 7, $\ln(\text{GSD})=0.3$, a median value of 7, an AM of 7.3 (Figure 4). This gave k_b with a range of 5×10^{-12} and 2×10^{-8} m/s, a median value of 2.4×10^{-10} m/s, and an AM of 4.9×10^{-10} m/s.

Table 2. Parameters used in modelling observed leakage with GMB/GCL composite liner.

Parameter	Unit	Distribution	a_o	GM	$\ln(\text{GSD})$	Figure
k_a (GCL)	m/s	Lognormal	0	3×10^{-11}	1.15	3
$(k_b/k_a) - 1$	-	Lognormal	-	7	0.3	4
θ	m^2/s		1×10^{-12}	3.2×10^{-11}	1.3	5

Liner thickness: $D=0.007$ m for GCL

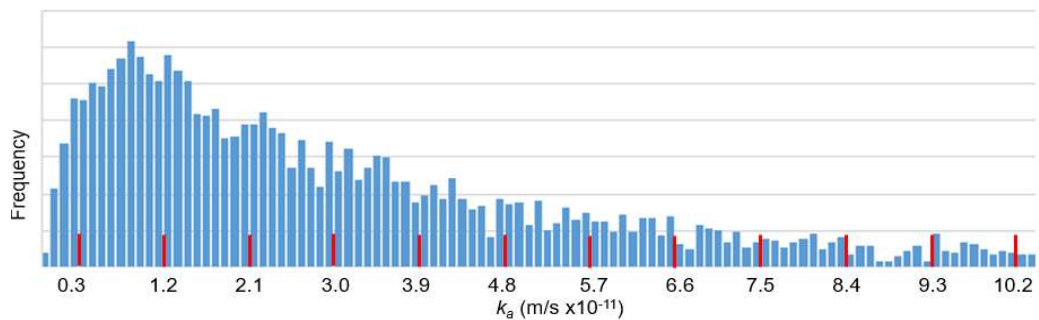


Figure 3. Frequency distribution for k_a (m/s) for GCL away from wrinkle

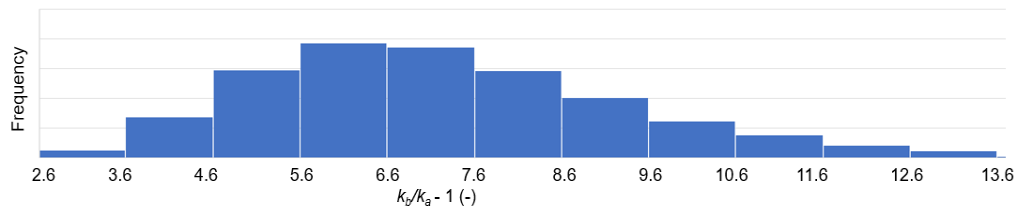


Figure 4. Frequency distribution for $[k_b/k_a - 1]$ (-) for GCL below wrinkle

GMB/GCL interface transmissivity, θ , had a range between 1×10^{-12} and 2×10^{-9} m^2/s , a median value of 3.3×10^{-11} m^2/s , an average of 7.5×10^{-11} m^2/s , and a distribution as shown in Figure 5.

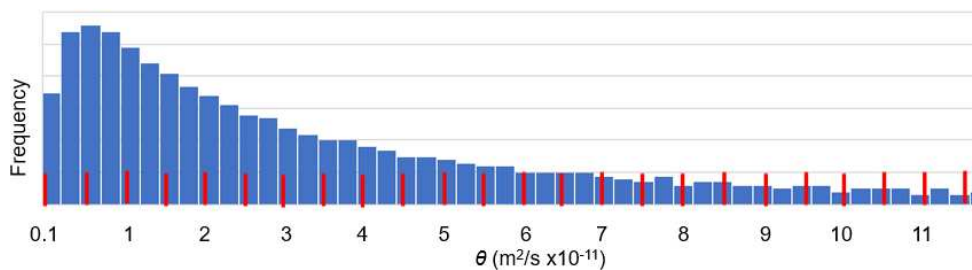


Figure 5. Frequency distribution for θ (m/s) for GMB/ GCL

3.3 CCL Parameters to fit observed data.

The best GMB/CCL composite liner parameters (Table 4) yielded distributions with the characteristics indicated in Table 3 for the CCL. The same parameters for the CCL (Table 4) were used both without and with an ELLS. Any water due to CCL consolidation is not modelled. The values of k_a and k_b were

each about an order of magnitude higher for the CCL than for the GCL while the interface transmissivity had a median value two orders of magnitude higher with the CCL than the GCL.

Table 3. Characteristics of the distributions resulting from parameters in Tables 2 and 4.

Parameter	Unit	GCL			CCL		
		Range	Median	AM	Range	Median	AM
k_a	m/s	9×10^{-13} - 1×10^{-9}	3×10^{-11}	5.8×10^{-11}	2×10^{-12} - 4×10^{-8}	2.5×10^{-10}	7.7×10^{-10}
k_b	-	5×10^{-12} - 2×10^{-8}	2.4×10^{-10}	4.9×10^{-10}	5×10^{-12} - 7×10^{-8}	5.1×10^{-10}	1.5×10^{-9}
θ	m ² /s	1×10^{-12} - 2×10^{-9}	3.3×10^{-11}	7.5×10^{-11}	1×10^{-10} - 7×10^{-8}	1.7×10^{-9}	3.3×10^{-9}

Table 4. Parameters used in modelling observed leakage with GMB/CCL composite liner.

Parameter	Unit	Distribution	a_o	GM	ln(GSD)
k_a (CCL)	m/s	Lognormal	0	2.5×10^{-10}	1.5
$(k_b/k_a) - 1$	-	Lognormal	-	1	0.05
θ	m ² /s		1×10^{-10}	1.6×10^{-9}	1.2

Liner thickness: D=0.6 m for GCL

3.4 Wrinkle parameters to fit observed data.

The input parameters for differential head, Δh , given in Table 5 yielded the distribution shown in Figure 6 with an AM of 0.2 m, standard deviation of 0.03 m, a minimum of 0.13 m with very few values more than 0.3 m. The distribution was the same except for the thickness of the clay liner where in both cases the head was assumed to be zero at the bottom of the liner.

Table 5. Head and wrinkle parameters used in modelling observed leakage.

Parameter	Unit	Distribution	a_o	GM	ln(GSD)
Δh (GCL)	m	Lognormal	0.1	0.1	0.3
Δh (CCL)	m	Lognormal	0.1	0.1	0.3
$2b$	m	Lognormal	0.1	0.1	0.1
			Minimum	Mode	Maximum
L_w (no ELLS)	m	Triangular	20	250	1450
L_w (with ELLS)	m	Triangular	0	20	1450

The same input parameters for the wrinkle width, $2b$, were used for composite liners with a GCL and CCL (Table 5). These parameters gave an average width of 0.2 m with a standard deviation of 0.01 m and range of 0.17-0.24m (Figure 7). A sensitivity analysis was performed with average width of 0.2 m with a standard deviation of 0.04 m and range of 0.12-0.54m with less than 3% effect on average leakage and no discernible effect on the plots shown in Figures 1 or 2.

The same length, L_w , of a wrinkle with a hole was used for both a GMB over a GCL and a CCL (Table 5). However, different distributions of wrinkle length were needed with and without an ELLS. With no ELLS the best fits to the data were obtained with holed wrinkles having a minimum length of 20 m, a mode of 250 m and a maximum of 1450 m. This distribution gave a 520 m-long median and 570 m-long AM holed wrinkle. Using the average values in Table 3 the wrinkle length required to give the arithmetic and geometric mean of the observed leakage with no ELLS was about 415 ± 35 m and 220 ± 20 m.

With a dipole ELLS, the best fits to the data were obtained with holed wrinkles having a minimum length of 0 m, a mode of 20 m and a maximum of 1450m. This distribution gave a median and AM wrinkle with

a hole of 430 m and 490 m, respectively. Using the average values in Table 3 the wrinkle length required to give the arithmetic and geometric mean of the observed leakage with a dipole ELLS was about 200 ± 20 m and 135 ± 15 m, respectively (i.e., about half that with no ELLS). When calculating leakages using Monte Carlo, outliers were rejected based on Chauvenet's criterion.

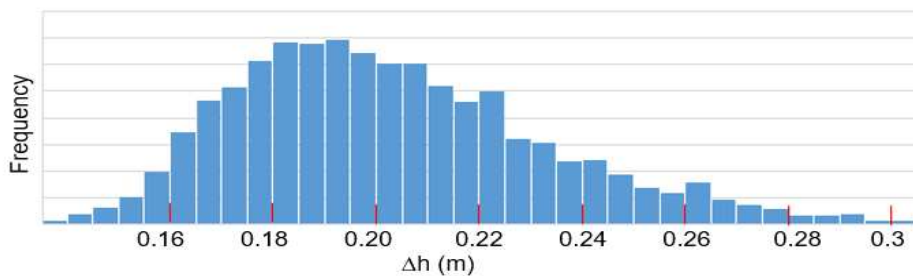


Figure 6. Frequency distribution for differential head, Δh (m)

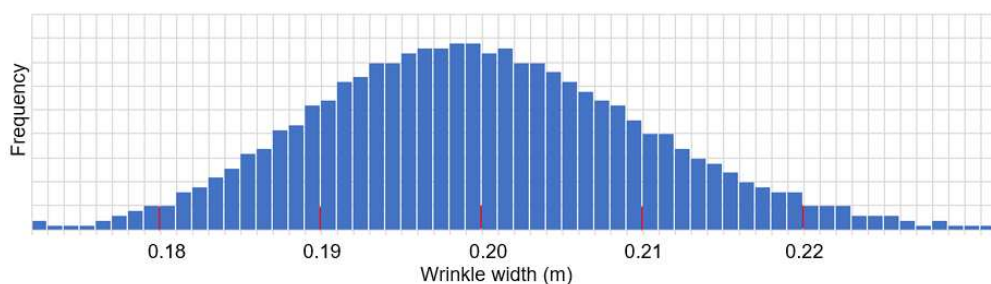


Figure 7. Frequency distribution for wrinkle width $2b$ (m)

4 ONTARIO GENERIC SINGLE-LINER DESIGN

The Province of Ontario, Canada, has a generic single-liner design that may be used for small landfills (MoE 1998) comprised of a GMB over a 0.75 m-thick CCL over a 3 m-thick attenuation layer (AL). This can be replaced by a GMB over a GCL over a ~3.75 m-thick attenuation layer (AL) provided leakage from the latter design can be shown to be smaller than for the former. Calculations were performed for this case using the calibrated parameters in Tables 2 and 4, and the wrinkle characteristics in Table 5. With a design leachate head of 0.3 m and potentiometric surface located a distance h_a above the bottom of the attenuation layer, the head drop across the system, Δh , could range between 0.3 m ($h_a = 3.75$) and 2.05 m ($h_a = 2$ m). If $h_a = 3$ m then $\Delta h = 1.05$. Considering a triangular distribution for Δh (minimum, mode, maximum) of $\langle 0.3, 1.05, 2.05 \rangle$ m in Table 6a and $\Delta h = \langle 0, 0.75, 1.75 \rangle$ m in Table 6b and 6c.

Three cases with a wrinkle having a hole of length L_w (m) were examined. The case with no ELLS and good construction quality assurance (CQA) were modelled with a triangular distribution for holed wrinkle length $L_w = \langle 20, 250, 1450 \rangle$ m. The case with an ELLS and good CQA were modelled with $L_w = \langle 0, 20, 1450 \rangle$ m. A case with very high quality CQA and a limitation on the time of the day wrinkles were covered such that no wrinkle exceeded 250 m when covered, were modelled with $L_w = \langle 0, 20, 250 \rangle$ m. The calculated leakage characteristics were as given in Table 6 which reports the AM and GM of leakages together with the median leakage and the leakage, Q_{95} , where there is a 95% probability the leakage will be less than Q_{95} . The GM and median values tend to be close together and may be regarded as the best measure of central tendency. The AM is typically much higher and is influenced by a few large leakage values. In most cases Q_{95} is quite large and reflects the broad distribution of leakage values given the variability of the many factors contributing to the leakage.

The results in Table 6 with $\Delta h = \langle 0.3, 1.05, 2.05 \rangle$ and $\Delta h = \langle 0, 0.75, 1.75 \rangle$ m all gave high leakages when the GCL was directly above the attenuation layer due to the relatively high suctions that developed with the water table well below the GCL combined with the assumption that the hydraulic conductivity of the AL was not directly affected by the suction. This is a very conservative assumption. The calculated leakage would likely be much lower if relationship between suction and k_{AL} of the AL was known. Even assuming k_{AL} has a GM and median = 1×10^{-7} m/s, $\ln(\text{DSD}) = 1.15$, the case with excellent construction

quality assurance limiting $L_w \leq 250\text{m}$ gave leakages warranting a contaminant transport calculation to verify whether or not the impact would be acceptable.

Table 6. Leakage through primary liner (GMB/GCL or GMB/CCL based on calibrated parameters as per Tables 2, 4, & 5)

	(a) Clay liner	Δh (m)			ELLS	CQA	Q, Leakage (lphd)			
		Min.	Mode	Max.			AM	GM	Median	Q_{95}
1	GCL	0.3	1.05	2.05	No ¹	Good ¹	485	252	263	1800
2	GCL	0.3	1.05	2.05	Yes ²	Good ²	415	181	204	1540
3	CCL	0.3	1.05	2.05	No ¹	Good ¹	148	77	82	570
4	GCL	0.3	1.05	2.05	Yes ³	Excellent ³	70	36	40	270
5	CCL	0.3	1.05	2.05	Yes ²	Good ²	133	56	62	500
6	CCL	0.3	1.05	2.05	Yes ³	Excellent ³	23	11	12	90
	(b) Clay liner	Min.	Mode	Max.	ELLS	CQA	AM	GM	Median	Q_{95}
7	GCL	0	0.75	1.75	No ¹	Good ¹	328	172	183	1330
8	GCL	0	0.75	1.75	Yes ²	Good ²	304	128	146	1150
9	GCL	0	0.75	1.75	Yes ³	Excellent ³	59	26	27	226
	(c) Clay liner	Min.	Mode	Max.	ELLS	CQA	AM	GM	Median	Q_{95}
10	GCL	0	0.75	1.75	No ¹	Good ¹	328	172	183	1330
111	CCL	0	0.75	1.75	No ¹	Good ¹	118	54	54	463
12	GCL+CCL	0	0.75	1.75	No ¹	Good ¹	28	12	13	113
13	GCL+CCL	0	0.75	1.75	Yes ²	Good ²	23	9	10	95
14	GCL+CCL	0	0.75	1.75	Yes ³	Excellent ³	9.3	4.2	4.4	37

¹ $L_w = <20, 250, 1450>$ m; ² $L_w = <0, 20, 1450>$ m; ³ $L_w = <0, 20, 250>$ m

k_{AL} : GM and median = 1×10^{-7} m/s; $\ln(\text{GSD})=1.15$; AM = 1.9×10^{-7} m/s; Range = 2.4×10^{-9} to 3.7×10^{-6} m/s

The situation was somewhat better for the thicker CCL but the leakages were still relatively large both with and without an ELLS except that the case with $L_w \leq 250\text{m}$ had leakages low enough to warrant a contaminant transport calculation.

The case where a GCL was combined with a CCL over the attenuation layer provided the best results a single-liner system, showing a potential benefit of combining a GMB + GCL+ CCL as a liner system. All the distributions of L_w gave encouragingly low AM, GM, and median values. However, even for these cases, Q_{95} was sufficiently high to warrant a contaminant transport calculation to ascertain the likely impact on an underlying aquifer.

Based on the deterministic values modelled by Rowe and Barakat (2021) and plotted in Figure 8, the allowable limits will be exceeded for leakage, i.e., (allowable limits, leakage for exceedance) for USA-EPA (4 ug/L, 0), Australia (70 ug/L, 20 lphd), Europe (100 ug/L, 30 lphd), Ontario (150 ug/L, 45 lphd), British Columbia (300 ug/L, 80 lphd) and rest of Canada (600 ug/L, 180 lphd). Comparing the leakages for exceedance with the geometric mean (GM) and median values calculated in Table 6, only the single liner system with GMB+CCL and both an ELLS and excellent CQA or a GMB+GCL+CCL would meet all regulatory requirements except USA. Only 43% of the scenarios would meet Ontario's requirements based on the median value. However, only 50% of cases would be below the median value. If a conservative approach were taking requiring 95% of predicted leakages to meet regulatory requirements (i.e., $Q < Q_{95}$), then none would meet USA, Australia, or Europe requirements, and only one (GMB+GCL+CCL and both an ELLS and excellent CQA) would meet Ontario's or British Columbia's requirements. Even the much less restrictive rest of Canada criterion would only be met in 28% of the cases examined based Q_{95} for PFOS for the cases examined here and by Rowe and Barakat (2021).

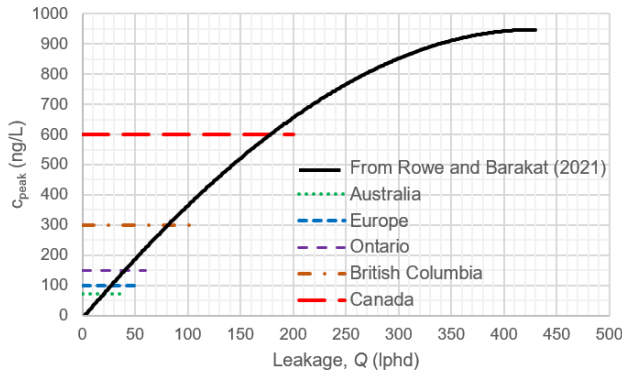


Figure 8. Peak PFOS impact in aquifer for different levels of leakage and regulatory limits.

5 DOUBLE COMPOSITE LINER PERFORMANCE

Using the calibrated parameters developed in the previous section, the leakage through a primary liner and a secondary liner in a double-lined system, with a leak detection and collection layer between the liners, was performed as described earlier assuming a similar wrinkle network and parameters for both the primary (GMB/GCL or GMB/CCL) and secondary liner (GMB/GCL + 1.743m AL) or (GMB/CCL + 1m AL) where the attenuation layer, AL, had $k_{AL} = 1 \times 10^{-7}$ m/s. The GCL and CCL had the same characteristics as indicated in Tables 2 and 4, respectively. The leachate level on the primary liner was as given in Table 5. For the secondary liner, the water table was assumed to be at an average elevation 0.15 m below the top of the attenuation layer and varied with a GM= 0.15 m and standard deviation $\ln(\text{GSD}) = 0.5$ in both cases. Thus, the results in Table 7 for the GCL represents an AM $\Delta h_{\text{secondary}} = 0.33$ m for the secondary liner, almost twice the AM $\Delta h_{\text{primary}} = 0.17$ m for the primary liner in acknowledgement of the uncertainty and variability of water levels below the secondary geomembrane. The arithmetic mean (AM) and geometric mean (GM) leakages together with the median leakage and Q_{95} are summarized in Table 7 for both the primary and secondary liner.

Table 7. Leakage through primary liner (GMB/GCL or GMB/CCL as per Tables 2, 4, & 5) and secondary line for $\Delta h_{\text{secondary}} = 0.15 + \exp(\text{NORM.INV}(), \ln(0.15), 0.5)$

Case	Secondary liner system below GMB	ELLS	CQA	Primary liner leakage (lphd)				Secondary liner leakage (lphd)			
				AM	GM	Med	Q_{95}	AM	GM	Med	Q_{95}
Primary Liner GMB/GCL: $\Delta h_{\text{primary}} = 0.1 + \exp(\text{NORM.INV}(), \ln(0.1), 0.3)$ m											
1	GCL ⁴ +1.75m AL	No ¹	Good ¹	140	66	67	575	48	33	35	150
2	GCL ⁴ +1.75m AL	Yes ²	Good ²	132	51	51	500	38	21	24	130
3	GCL ⁴ +1.75m AL	Yes ³	Excellent ³	20	9	10	90	7	4	5	23
Primary Liner GMB/CCL: $\Delta h_{\text{primary}} = 0.1 + \exp(\text{NORM.INV}(), \ln(0.1), 0.3)$ m											
4	CCL ⁵ + 1 m AL	No ¹	Good ¹	120	64	62	430	54	35	37	175
5	CCL ⁵ + 1 m AL	Yes ²	Good ²	100	46	49	380	44	23	26	140
6	CCL ⁵ + 1 m AL	Yes ³	Excellent ³	20	10	11	70	8	5	5	27
Primary Liner GMB/GCL: $\Delta h_{\text{primary}} = 0.1 + \exp(\text{NORM.INV}(), \ln(0.1), 0.3)$ m											
7	GCL ⁴ +CCL ⁵ + 1 m AL	No ¹	Good ¹	140	67	69	575	22	13	13	73
8	GCL ⁴ +CCL ⁵ + 1 m AL	Yes ²	Good ²	132	51	51	500	17	8	9	62
9	GCL ⁴ +CCL ⁵ + 1 m AL	Yes ³	Excellent ³	20	9	10	90	3	2	2	11

¹ $L_w (20, 250, 1450)$; ² $L_w (0, 20, 1450)$; ³ $L_w (0, 20, 250)$; ⁴ GCL 0.007m thick, ⁵ CCL 0.75 m thick

For the Ontario single-liner, the CCL+AL was more effective than the GCL+AL whereas in the double-liner system the opposite was true. The leakage through the secondary liners were small (< 10 lphd) for

all cases with CQA and a contract that limited wrinkles at the time of covering to less than 250 m. Comparison the potential leakage to the environment with the single (Table 6) and double-lined system for Ontario landfills (Table 7) makes a very clear point as to why Ontario requires a double-liner for all but very small landfills. Table 6 and 7 and Figure 8 highlight the importance of excellent CQA and not covering the GMB while there are significant wrinkles.

4. CONCLUSIONS

Based on the observed leakage through 182 landfill cells with good quality assurance (122 with no electrical leak location survey and 60 with a dipole leak location survey), the parameters controlling leakage through composite liners with both a GCL and CCL were established. The same parameters were used both with and without the leak location survey for liner materials and the only difference was the length of wrinkles with holes, L_w , that remained with and without the ELLS. These parameters were then used to predict the leakage through Ontario's single composite liner system considering uncertainty with respect to the location water table within the attenuation layer. It is shown that the leakages, while likely acceptable for contaminants of concern in the last century, warrant serious further consideration for leachate containing PFAS. In contrast, the leakage through the secondary liner of the Ontario double-liner system is very small with the use of a GCL and modest, but substantially lower than with a single-lined system, with a CCL. The results suggest the value of a composite liner with both a GCL and CCL. The results also indicate that more work is required to assess the likelihood of PFAS in leachate causing an unacceptable problem in the future with existing single-lined facilities.

5. ACKNOWLEDGEMENTS

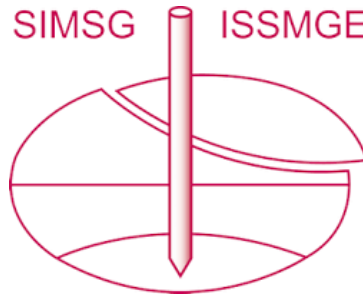
Funding for this work was provided by the Australian Research Council Linkage grant (LP180101178) and Natural Sciences and Engineering Research Council grant RGPIN-2022-03928.

REFERENCES

- Beck, A. 2015. "Available technologies to approach zero leaks." In Proc., of the Geosynthetics 2015 Conf. Roseville, CA: Industrial Fabrics Association International.
- Brachman, R.W.I., Gudina, S. 2008. Geomembrane strains and wrinkle deformations in a GM/GCL composite liner. *Geotext. Geomembr.*, 26 (6), 488-497.
- Chappel, M.J., Brachman, R.W.I., Take, W.A. and Rowe, R.K. 2012a. Large-scale quantification of wrinkles in a smooth, black, HDPE geomembrane, *ASCE J. Geotech. & Geoenvironl Engineering*, 138 (6): 671-679.
- Chappel, M.J., Rowe, R.K., Brachman, R.W.I. and Take, W.A. 2012b. A comparison of geomembrane wrinkles for nine field cases. *Geosynthetics International*, 19(6): 453-469.
- Di Battista, V., Rowe, R.K., Patch, D., Weber, K., 2020. PFOA and PFOS Diffusion through Geomembranes at Multiple Temperatures. *Waste Manage.* 117, 93–103. <https://doi.org/10.1016/j.wasman.2020.07.036>.
- El-Zein, A. and Balaam, N. 2012. Saturated-unsaturated flow and solute transport in engineered liner systems: a new special-purpose finite-element analysis software. *Australian Geomechanics Journal*, 47(3):11-126.
- Gilson-Beck, A. 2019. Controlling leakage through installed geomembranes. *Geotext. Geomembr.* 47 (5): 697–710.
- Gudina, S., Brachman, R.W.I. 2006. Physical response of geomembrane wrinkles overlying compacted clay, *Journal of Geotechnical and Geoenvironmental Engineering*, 132(10): 1346-1353.
- Gudina, S., and Brachman, R. W. I. 2011. Geomembrane strains from wrinkle deformations. *Geotext. Geomembr.* 29(2): 181-189.
- MoE. 1998. Ontario Regulation 232/98: Landfilling Sites, Environmental Protection Act, 1990. Govt. of Ontario.
- Rowe, R.K. 2020. Protecting the environment with geosynthetics - The 53rd Karl Terzaghi Lecture. *ASCE J Geotech. Geoenviron.*, 146(9):04020081, 10.1061/(ASCE)GT.1943-5606.0002239
- Rowe, R.K. and Barakat, F.B. (2021) "Modelling the transport of PFOS from single lined municipal solid waste landfill", *Computers and Geotechnics*, 137(9):104280-1 104280-11.
- Rowe, R.K., Quigley, R.M., Brachman, R.W.I. and Booker, J.R. 2004. *Barrier Systems for Waste Disposal Facilities*, E & FN Spon, Taylor & Francis Books Ltd, London, 587p.
- Rowe, R.K., Chappel, M.J., Brachman, R.W.I. and Take, W.A. (2012a). "Field monitoring of geomembrane wrinkles at a composite liner test site", *Canadian Geotechnical Journal*, 49(10): 1196-1211.

- Rowe, R.K., Yang, P., Chappel, M.J., Brachman, R.W.I. and Take, W.A. (2012b). "Wrinkling of a geomembrane on a compacted clay liner on a slope", *Geotechnical Engineering, J. South East Asian Geotech. Soc.*, 43(3): 11-18.
- Take, W.A., Chappel, M.J., Brachman, R.W.I, Rowe, R.K. 2007. Quantifying geomembrane wrinkles using aerial photography and digital image processing. *Geosynthetics International* 14 (4), 219-227

INTERNATIONAL SOCIETY FOR SOIL MECHANICS AND GEOTECHNICAL ENGINEERING



This paper was downloaded from the Online Library of the International Society for Soil Mechanics and Geotechnical Engineering (ISSMGE). The library is available here:

<https://www.issmge.org/publications/online-library>

This is an open-access database that archives thousands of papers published under the Auspices of the ISSMGE and maintained by the Innovation and Development Committee of ISSMGE.

The paper was published in the proceedings of the 9th International Congress on Environmental Geotechnics (9ICEG), Volume 1, and was edited by Tugce Baser, Arvin Farid, Xunchang Fei and Dimitrios Zekkos. The conference was held from June 25th to June 28th 2023 in Chania, Crete, Greece.